Journal of Computational and Applied Mathematics 235 (2011) 1941–1955

Contents lists available at ScienceDirect

Journal of Computational and Applied Mathematics

journal homepage: www.elsevier.com/locate/cam

New series for the cosine lemniscate function and the polynomialization of the lemniscate integral

John P. Boyd *

Department of Atmospheric, Oceanic and Space Science and Laboratory for Scientific Computation, University of Michigan, 2455 Hayward Avenue, Ann Arbor, MI 48109, United States

ARTICLE INFO

Article history:
Received 9 January 2010
Received in revised form 17 September 2010

Keywords:
Elliptic functions
Imbricate series
Lemniscate integral
Lemniscate cosine

ABSTRACT

We discuss the numerical computation of the cosine lemniscate function and its inverse, the lemniscate integral. These were previously studied by Bernoulli, Euler, Gauss, Abel, Jacobi and Ramanujan. We review general elliptic formulas for this special case and provide some novelties. We show that a Fourier series by Ramanujan converges twice as fast as the standard elliptic cosine Fourier series specialized to this case. The so-called imbricate series, however, converges geometrically fast over the entire complex plane. We derive two new expansions. The rational-plus-Fourier series converges much faster than Ramanujan's: for real z: each term is asymptotically 12,400 times smaller than its immediate predecessor: $\mathrm{coslem}(z) = 4B\,\{\sqrt{q}(1-q)\cos(Bz)/[(1+q)^2 - 4q\cos^2(Bz)] + \sum_{n=1}^{\infty} q^{n-1/2}\{1/(1+q^{2n-1}) - 1\}\cos((2n-1)Bz)\}$ where $q = \exp(-\pi)$ is the elliptic nome, $K \approx 1.85\ldots$ is the complete elliptic integral of the first kind for a modulus $m = 1/2$ and $B = \pi/(K\sqrt{2})$. The rational imbricate series is uniformly valid over the complex plane, but converges twice as fast as the sech-imbricate series: $\mathrm{coslem}(z) = 4B\sqrt{q}(1-q)\sum_{j=-\infty}^{\infty}\sqrt{q}(1-q)\cos(Bz)/\{(1+q)^2 - 4q\cos^2(B[z - jP\,i])\}$ where $P = (4/\sqrt{2})K$ is the period in both the real and imaginary directions.

We devise a new approximation for the lemniscate integral for real argument as the arccosine of a Chebyshev series and show that 17 terms yield about 15 digits of accuracy. For complex argument, we show that the lemniscate integral can be found to near machine precision (assumed as sixteen decimal digits) by computing the roots of a polynomial of degree thirteen. Alternatively, Newton's iteration converges in three iterations with an initialization, accurate to four decimal places, that is the chosen root of a cubic equation.

> [Of the lemniscate integral] "I have strong grounds to believe that the construction of our curve depends neither on the quadrature nor on the rectification of any conic section".
>
> James Bernoulli (1694)

1. Introduction

In this article, we offer some new formulas for numerical evaluation of an important special case of the elliptic functions. We also provide a modern numerical perspective on some old expansions.

* Tel.: +1 734 764 3338.
E-mail addresses: jpboyd@engin.umich.edu, j.p.boyd@comcast.net.
URL: http://www.engin.umich.edu/~jpboyd/.

0377-0427/$ – see front matter © 2010 Elsevier B.V. All rights reserved.
doi:10.1016/j.cam.2010.09.020

1.1. Bernoulli, Euler, Gauss and all that

James Bernoulli studied the lemniscate integral in 1694. The function was then dubbed the "curva elastica" because it arose in elasticity theory. Count Giulio Fagnano (1682–1766) derived an addition theorem for this function in 1718, reproduced as (58). He was so proud of his work on the lemniscate – this identity and his procedure for subdividing the curve with ruler and compass – that the title page of his collected works displays an engraving of the lemniscate with the words "Multifariam divisa atque dimensa Deo veritatis gloria", and he repeated the curve on his tomb. Leonard Euler (1707–1783), asked to examine the Count's collected papers after he was recommended for membership in the Berlin Academy in 1751, was inspired to simplify and extend Fagnano's work, yielding (59), and moving Jacobi nearly a century later to date this moment as the "birth of elliptic functions".

Carl Gauss in 1797 defined the inverse of the lemniscate integral as the "cosine lemniscate" function plus a similar "sine lemniscate" function. He derived many identities among these functions. He was apparently the first to understand that the easiest way to understand the elliptic *integrals* is through their *inverses*, which are the elliptic analogues of the usual sine and cosine, etc.

Gauss published only a part of his work, more hints than conclusions. Niels Henrik Abel and Carl Gustav Jacobi in the 1820s realized, as had Gauss, that the key to understand the lemniscate integral was to first understand the cosine lemniscate function (page 186 of [1]).

Ayoub [2], Scarpello and Ritelli [3], Sridharan [4,5], Rice [6] and Levien [7] give good summaries of this ancient history. Legendre first obtained the analytical formula for the complete elliptic integral of the first kind for the lemniscate case

$$K(m = 1/2) = \frac{1}{4}\frac{1}{\sqrt{\pi}}\{\Gamma(1/4)\}^2 = 1.854074677301371918\ldots. \tag{1}$$

The cosine lemniscate and sine lemniscate functions both conformally map a diamond-shaped region to a unit disk. This is a special case of the Schwarz–Christoffel mapping [8]. Indeed, the earliest published drawing of a Schwarz–Christoffel transformation was precisely of the lemniscate map in Schwarz' very first paper [9], reproduced as Figure 1.4 of [8]. Modern applications of the square-to-disk map include [10–12].

In 1879, Charles Peirce employed the lemniscate functions in his "quincuncial" projection which maps the surface of a sphere conformally to a square [13]. The French cartographer Emile Guyou in 1887 and the American Oscar Adams in 1925 devised similar sphere-to-square projections [14]. These three projections, although distinct, are transverse projections of one another [15,16].

Ramanujan gave ten identities for the lemniscate functions in his notebooks (without proof, as was his custom); these are all proved in [17]. Ramanujan's first series for the cosine lemniscate function converges much faster than the classical Fourier series as described below—but not as fast as the rational-plus-Fourier expansion derived here for the first time.

The lemniscate case is given an entire page in the *NBS Handbook of Mathematical Functions* [18], but only in the context of Weierstrass elliptic functions. The half-period, $P/2$ in our notation, is dubbed the "lemniscate constant" and given to eighteen decimal places.

Applications of lemniscate functions, just in the last three years, include Scarpello and Ritelli [3] [elasticity theory], Leble [19] [quantum sine-Gordon generalizations] and Kurt [10], Amore [11] and Boyd and Yu [12] [Poisson or Helmholtz equations in a disk or square, which requires lemniscate functions of complex argument].

1.2. Basic definitions

Gauss himself used 'cl' and 'sl' for the cosine and sine lemniscates functions, but we prefer the notation of Ayoub [2] to avoid confusion with the standard notation for the Clausen functions.

The lemniscate integral is

$$\text{arccoslem}(w) = \int_w^1 \frac{1}{\sqrt{1-t^4}}\,\mathrm{d}t. \tag{2}$$

Gauss defined the cosine lemniscate function as the inverse of the lemniscate integral, but it is more convenient to equivalently define the function as a special case of the elliptic cosine function:

$$\text{coslem}(z) = \text{cn}(\sqrt{2}z;\, m = 1/2) \tag{3}$$

where the period of $\text{cn}(u;\, m = 1/2)$ is $4K$ in u.

The sine lemniscate function is just the translation of the cosine lemniscate function:

$$\text{sinlem}(z) = \text{coslem}(z - P/4) \tag{4}$$

where $P = 5.244\ldots$ is the spatial period of the lemniscate functions. Consequently, it is unnecessary to treat the sine lemniscate function in detail. It can be defined directly as

$$\text{sinlem}(z) = \frac{1}{\sqrt{2}}\,\frac{\text{sn}(\sqrt{2}z;\, m = 1/2)}{\text{dn}(\sqrt{2}z;\, m = 1/2)} \tag{5}$$

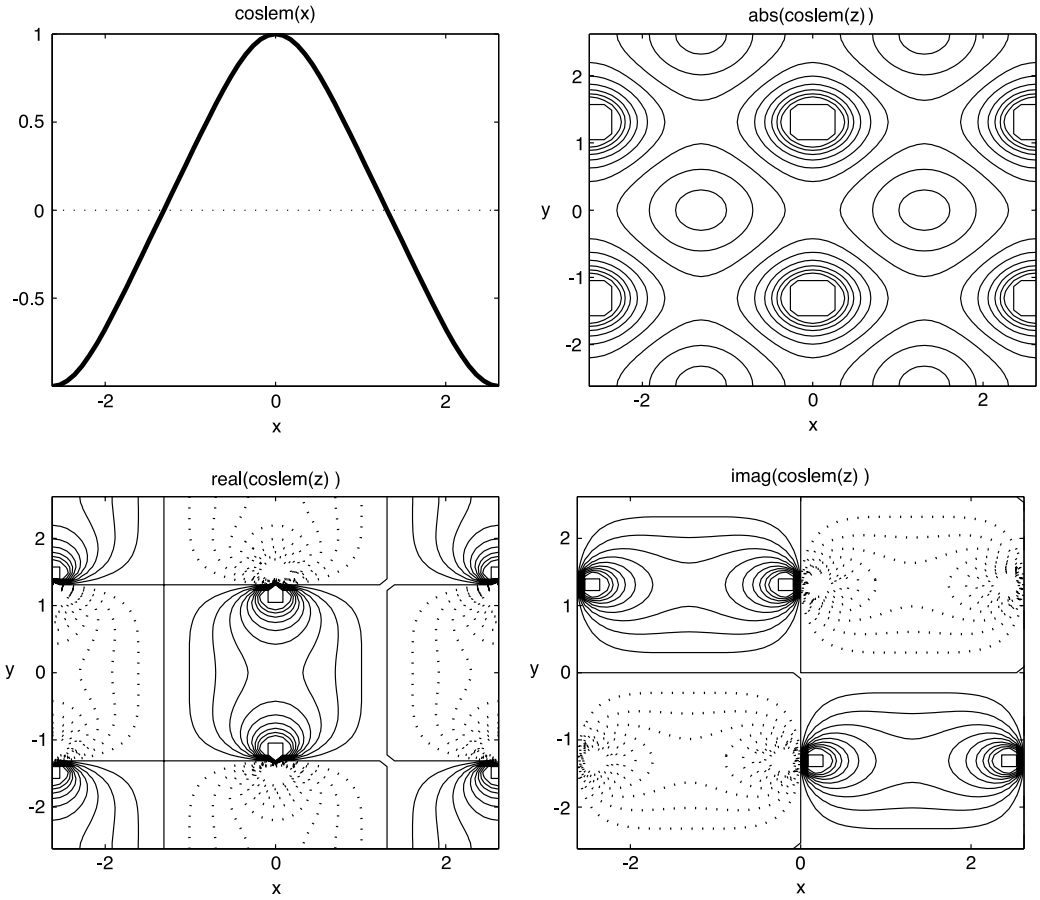

Fig. 1. Upper left: coslem(x) for real x on $x \in [-P/2, P/2]$ where $P \approx 5.244$ is the spatial period. Upper right: absolute value of the same function on $\Re(z) \in [-P/2, P/2]$, $\Im(z) \in [-P/2, P/2]$. Contours 0:3:0.3:3. Lower panels: same but for the real and imaginary parts with contours -3:0.3:3. Negative-valued contours are dashed.

with the inverse

$$\text{arcsinlem}(w) = \int_0^w \frac{1}{\sqrt{1-t^4}}\mathrm{d}t. \tag{6}$$

The contour plots in Fig. 1 show that the cosine lemniscate function has many symmetries in the complex plane. These symmetries can be deduced from the Fourier series for the function plus the identity $\cos(x + \mathrm{i}y) = \cos(x)\cosh(y) - \mathrm{i}\sin(x)\sinh(y)$. The real part of the cosine lemniscate function is symmetric with respect to the real and imaginary axes while the imaginary part is antisymmetric with respect to both axes. The real part is also antisymmetric with respect to $\Re(z) = \pm P/4$ and $\Im(z) = \pm \mathrm{i}P/4$ while the imaginary part of coslem(z) is symmetric with respect to $\Re(z) = \pm P/4$ and $\Im(z) = \pm \mathrm{i}P/4$. Because of all these symmetries, it is possible to deduce the function in the entire period box from knowledge of its values in the square with vertices at $(0, 0)$, $(0, P/4)$, $(P/4, 0)$, $(P/4, P/4)$ which occupies only $1/16$ of the area of the period box.

The cosine and sine lemniscate function and their inverses satisfy many identities. Since we have not seen these collected in one place, we have cataloged these in the Appendix.

1.3. Why the cosine lemniscate function is special

1. Equal real and imaginary periods.
2. Fourier and imbricate series converge at identical rates for real x.
3. Equally well approximated by sine wave and soliton.
4. Special solutions for non-integrable wave equations.
5. The arcsinlem function has C_4 rotational symmetry in the complex plane; only every fourth term in its power series is nonzero.
6. Conformally maps the unit square to the unit disk.
7. Origin of elliptic functions.

Table 1
Lemniscate numerical parameters.

Symbol	Value	Name
m	$1/2$	Elliptic modulus
k	$1/\sqrt{2}$	Alternative modulus
q	$\exp(-\pi) = 0.0432139$	Elliptic nome
K	$\frac{1}{4}\frac{1}{\sqrt{\pi}}\{\Gamma(1/4)\}^2 = 1.854074677301371918$	Complete elliptic integral, 1st kind
P	$(4/\sqrt{2})K = 5.24411510858423962$	Period
A	$2\sqrt{2}\pi/K\sqrt{q}(1-q) = 0.95322256797153$	Amplitude of rational functions
B	$\pi/(\sqrt{2}K) = 1.198140234735592207$	$= (2\pi/P)$

All Jacobian elliptic functions $v(x, m)$ are periodic with a *real* period and an *imaginary* period so that $v(x + 4K(m)p + \mathrm{i}4K'(m)q, m) = v(x, m)$ for any integers p and q where $K(m)$ is the complete elliptic integral of the first kind of modulus m and $K'(m)$ is the complementary integral. The cosine lemniscate and sine lemniscate are the special case $m = 1/2$ for which $K(m) = K'(m)$ so that the real and imaginary periods are *identical*.

All Jacobian elliptic functions (for general modulus m) have both a Fourier series and an imbricate series where the latter is a sum of translated-but-otherwise-identical copies of a hyperbolic function [20]. These were known since the work of Eisenstein in the 1840s. The term "imbrication", borrowed from a Latin word meaning "to overlap like roof tiles", has become common in wave theory because of the great usefulness of such series in the study of solitary waves and their periodic generalizations as explained further in a moment.

When the elliptic modulus $m < 1/2$, the Fourier series converges faster than the imbricate series for *real* z; when $m > 1/2$, the imbricate series is faster. The lemniscate functions are the case where the Fourier and imbricate series both converge at an identical (fast) rate as discussed in detail below.

Many species of nonlinear waves are approximated by solutions to the Korteweg–deVries (KdV) and Nonlinear Schroedinger equations [21–23]. The elliptic function traveling waves are parameterized by the elliptic modulus over its full range $m \in [0, 1]$. Because the terms in the imbricate series are the shapes of the solitons, we have the remarkable fact that in the KdV case the "cnoidal" waves are the exact, nonlinear superposition of solitons as first noted by Toda [23]. The cnoidal waves are infinitesimal amplitude sine waves in the limit $m \to 0$ and are tall, narrow "solitons" in the limit $m \to 1$. (The alternative name "solitary waves" is misleading because a cnoidal wave with $m \approx 1$ is an infinite chain of identical tall peaks, narrow compared to the spatial period and "solitary" only in this sense of narrowness.) The cosine lemniscate waves – perhaps one could call them "lemniscoidal waves" – are the special case where the wave is both a sine wave and a soliton in equal measure. Boyd [24,25] showed that for the KdV lemniscoidal wave, the phase speed formulas based on the sine wave and the soliton both have errors of 4.7%. In other words, the lemniscate case is that in which the KdV traveling wave is both soliton and sine wave of equal degree. A similar analysis for the NLS wave is given in [26]. The soliton–sine wave connection is exploited for non-elliptic traveling waves in [27,28].

Generalizations of the KdV and NLS equations are usually "non-integrable" which means among things that the traveling waves are generally not elliptic functions. However, some of these have *special* solutions which are elliptic—almost always the cosine lemniscate function, perhaps raised to a power. Special traveling waves proportional to the fourth power of the cosine lemniscate function for $u_t + uu_x - u_{5x} = 0$ are given in [29,30]:

$$u_t + uu_x - u_{5x} = 0, \qquad u(x, t) = 420\, B^4 \mathrm{coslem}^4\left(B[x - 168\, B^4 t]\right). \tag{7}$$

Imbricate series are given as his (22) in [31].

Only every *fourth* term in the Taylor series is nonzero in the following:

$$\mathrm{arcsinlem}(w) = \sum_{n=0}^{\infty} \frac{(1/2)_n\, w^{4n+1}}{n!(4n+1)} = w\, {}_2F_1(1/4, 1/2, 5/4, w^4) \tag{8}$$

where $(1/2)_n$ is a Pochhammer symbol. This implies that $\mathrm{arcsinlem}(w)/w$ is invariant with respect to rotations about the origin by any multiple of $\pi/2$ in the complex w-plane.

The diamond-shape region with vertices at $z = (0, 0)$, $(K/\sqrt{2}, K/\sqrt{2})$, $(0, \sqrt{2}K)$ and $(K/\sqrt{2}, -K/\sqrt{2})$ where $K = 1.85407\ldots$ is mapped conformally to the unit disk in the w-plane by

$$[\text{disk}]\ w = \mathrm{coslem}(z) \quad [\text{diamond}]. \tag{9}$$

This map (with a rotation of the diamond) allows numerical software for the *square* to be applied to interpolation and differential equations in a *disk*-shaped domain [11,12] (Table 1).

Lastly, as noted earlier, the cosine lemniscate function and lemniscate integrals had a special, pioneering role in the history of elliptic functions and integrals. This has persisted into modern times: in his three-volume tome on complex variable theory and elliptic functions, Siegel devotes the first ten pages of the first volume to lemniscate integrals and their inverses, seeing this special case as an ideal introduction to the whole [32].

2. Numerical evaluation of the cosine lemniscate function

2.1. Classical Fourier and imbricate series

The cosine lemniscate function has five series representations: the standard Fourier series, the sech-imbricate series, a special Fourier series devised by Ramanujan (Theorem 2.1 of [17]), and two further expansions derived here for the first time.

The classical Fourier series is

$$\begin{aligned}\mathrm{coslem}(z) &= \frac{2\,\pi}{kK}\sum_{n=1}^{\infty}\frac{\exp(-\pi\,(n-1/2))}{1+\exp(-\pi\,(2n-1))}\,\cos\left((2n-1)\,B\,z\right) \quad \text{[Fourier]}\\ &= 4.79256\sum_{n=1}^{\infty}\frac{\exp(-\pi\,(n-1/2))}{1+\exp(-\pi\,(2n-1))}\,\cos\left((2n-1)1.1981402z\right)\end{aligned} \tag{10}$$

where

$$B\equiv\frac{\pi}{2\,K}\sqrt{2}. \tag{11}$$

An "imbricate" series is one which consists of an infinite series of translated copies of a "pattern" function; the general theory is reviewed in [25]. The classical imbricate series for elliptic functions are periodizations of the sech or tanh functions; in particular,

$$\begin{aligned}\mathrm{coslem}(z) &= \frac{\pi}{\sqrt{2}K}\sum_{m=-\infty}^{\infty}(-1)^m\ \mathrm{sech}(B(z-mP/2))\\ &= 1.1981402\sum_{m=-\infty}^{\infty}(-1)^m\ \mathrm{sech}(1.1981402(x-2.622057m))\end{aligned} \tag{12}$$

where the spatial period of lemniscate functions is

$$P\equiv\frac{4}{\sqrt{2}}K=5.24411510858423962. \tag{13}$$

As reviewed in Chapter 2 of [33], a Fourier series for a general function $f(x)$ converges within the largest strip $|\Im(z)|\le\mu$ which is free of singularities (poles, branch points, and jumps due to lack of periodicity). If μ is the half-width of the strip of convergence, then the Fourier coefficients a_n decrease proportionally to $\exp(-nB\mu)$. The terms $a_n\cos(nBz)$ decrease proportionally to $\exp(-nB[\mu-|\Im(z)|])$.

Recalling that $\mathrm{sech}(x+\mathrm{i}y)=1/\{\cosh(x)\cos(y)+\mathrm{i}\sinh(x)\sin(y)\}$, each hyperbolic secant function of the imbricate series has an infinite set of simple poles spaced evenly on the imaginary axis or on lines parallel to the imaginary axis. Therefore, the imbricate series converges *uniformly* throughout the *entire* complex plane. The sum as a whole includes the entire doubly infinite lattice of singularities of the cosine lemniscate function. We therefore employed the imbricate series to perform conformal mapping of a square in the complex plane to the unit disk in [12].

The Fourier series converges only within the strip $|\Im(z)|\le P/4$, limited by the infinite rows of poles on the lines $\Im(z)=\pm P/4\approx 1.31\ldots$. Consistent with the general theory, the coefficients of $\cos((2n-1)Bz)$ decrease proportionally to $\exp(-2B\mu n)=\exp(-2B(P/4)n)=\exp(-n\pi)$.

Every Jacobian elliptic function, of which the cosine lemniscate function is a special case, has both a Fourier series and an imbricate series [20]. As noted earlier, the cosine lemniscate function is peculiar in that both series converge at exactly the same rate for real x. All the even Fourier coefficients are zero; the coefficient of $\cos((2n-1)Bz)$ is proportional to the nth power of q, the elliptic nome, which for the lemniscate case is $q=\exp(-\pi)\approx 0.042$. Let us group a pair of terms for m and $-m$ in the imbricate series and regard the pair as a single term, which is reasonable since (i) these terms are of comparable magnitude and (ii) each cosine of the Fourier series is the sum of two complex conjugate exponentials. Then the mth term of the imbricate series is also proportional mth power of q. In the next subsection, we shall discuss an approximation due to Ramanujan which converges much faster for real x.

2.2. Ramanujan's series

$$\mathrm{coslem}(x)=\sigma(z)\frac{1}{B|\sqrt{\mathcal{R}(B(z+P/4))}|} \tag{14}$$

where $B=\pi/(\sqrt{2}K)$ and

$$\mathcal{R}(Bz)\equiv\csc^2(Bz)-\frac{1}{\pi}-8\sum_{n=1}^{\infty}\frac{n}{\exp(2n\pi)-1}\,\cos(2nBz) \tag{15}$$

$$\sigma(z)=\mathrm{sign}\left(\cos(\Re(Bz))\right)\mathrm{sign}\left(\cos(\Im(Bz))\right). \tag{16}$$

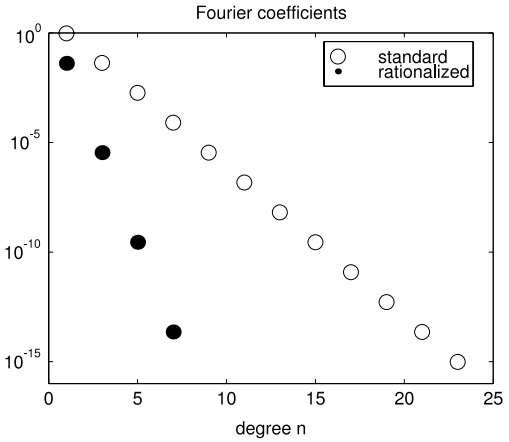

Fig. 2. Fourier coefficients for the classical Fourier series (open circles) and for the rational-plus-Fourier series (solid disks). The coefficients for Ramanujan's series, not shown, are halfway between the other two sets of coefficients. Note that only four terms in the rational-plus-Fourier series include all terms that are greater than machine epsilon (2.2×10^{-16}, the bottom of the graph) for real z.

The formula is discussed only as an expression for $\text{coslem}^2(z)$ in Ramanujan's notebook and in [17]; the σ factor, which is novel, correctly resolves the ambiguity in the sign of the square root.

The nth term of Ramanujan's series is proportional for large n to q^{2n}. It thus converges twice as fast as either of the two standard series for real z. It is remarkable that only 12 terms of the standard Fourier series or just six terms of Ramanujan's series suffice to evaluate the cosine lemniscate function to typical machine precision (2.2×10^{-16}) for all real z!

In the complex plane, the Fourier series converges within the strip which is bounded by the closest poles of the function at $z = \pm iP/4$ where P is the real spatial period. Ramanujan's series converges within a strip which is twice as wide, defined by $|\Im(z)| < P/2$. This miracle is possible because the poles in the cosecant function correctly approximate the poles of the cosine lemniscate function at $z = \pm iP/4$ and their images under the real periodicity.

In the next subsection, though, we shall offer a Fourier series that converges faster than Ramanujan's.

2.3. A rational-and-Fourier approximation

The author's book [33] uses the exemplary function $\lambda(z; p) \equiv (1-p^2)/\left\{(1+p^2) - 2p\cos(z)\right\}$, which has the delightfully simple Fourier series $\lambda(z; p) = 1 + 2\sum_{n=1}^{\infty} p^n \cos(nz)$. From this, we can construct a function with only odd cosines and coefficients that are powers of the parameter p:

$$\Lambda(z; p) \equiv p(1-p^2)\frac{\cos(z)}{(1+p^2)^2 - 4p^2\cos^2(z)} = \sum_{n=1}^{\infty} p^{2n-1}\cos([2n-1]z). \tag{17}$$

A common artifice for accelerating slowly converging series whose coefficients have an *asymptotic* form with a closed-form sum is to add the analytical sum while simultaneously subtracting its series. We can do this for the cosine lemniscate function by thus adding and subtracting $\Lambda(z; p = \exp(-\pi/2))$ to obtain

$$\begin{aligned}\text{coslem}(z) &= \frac{2\sqrt{2}\pi}{K}\sqrt{q}(1-q)\frac{\cos(Bz)}{(1+q)^2 - 4q\cos^2(Bz)} + \frac{2\sqrt{2}\pi}{K}\sum_{n=1}^{\infty} q^{n-1/2}\left\{\frac{1}{1+q^{2n-1}} - 1\right\} \\ &\quad \times \cos\left((2n-1)\frac{\pi}{\sqrt{2}\,K}z\right) \qquad (18) \\ &= 0.95322\,\frac{\cos(Bz)}{1.0883 - 0.17286\,\cos^2(Bz)} - 4B\sum_{n=1}^{\infty} q^{3n-3/2}\left\{\frac{1}{1+q^{2n-1}}\right\}\cos\left((2n-1)Bz\right). \qquad (19)\end{aligned}$$

The coefficients of the new Fourier series converge proportional to the *cube* of the nome: each term is smaller than its predecessor by a factor of 12,400! This is possible because $\Lambda(Bz; p = \exp(-\pi/2))$ includes all the poles of the cosine lemniscate function at $\Im(z) = \pm P/4$; the residual Fourier series for the *difference* $\text{coslem}(z) - \Lambda(Bz; p = \exp(-\pi/2))$ converges in a strip three times as wide (and three times as fast for real z), all the way to the next rows of poles at $\Im(z) = \pm 3P/4$. This implies that the coefficients of the new Fourier series fall proportionally to q^{3n} instead of q^n (Fig. 2).

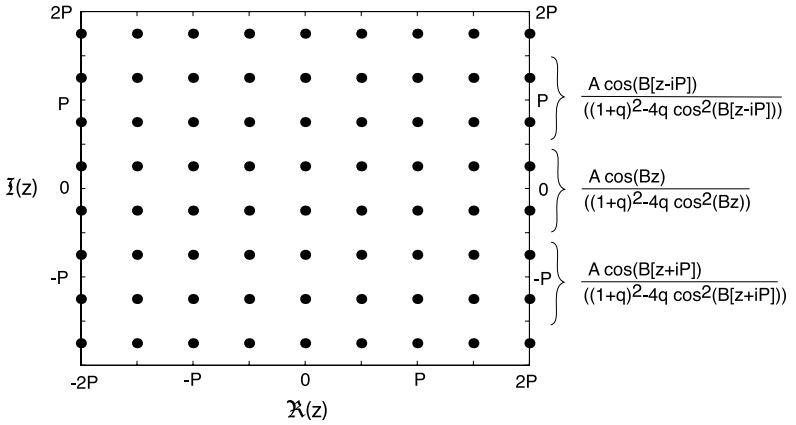

Fig. 3. The black circles depict part of the doubly infinite lattice of simple poles of the coslem function in the complex z-plane. P is the spatial period, the same in both the real and imaginary directions. The rational function $A\cos(Bz)/((1+q)^2-4q\cos^2(Bz))$ accounts for the rows of poles at $\Im(z)=\pm iP/2$. The $m=\pm1$ terms in the rational imbricate series similarly account for two horizontal rows of poles each. The sech-imbricate series converges more slowly because each sech accounts for only a *single* (vertical) row of poles.

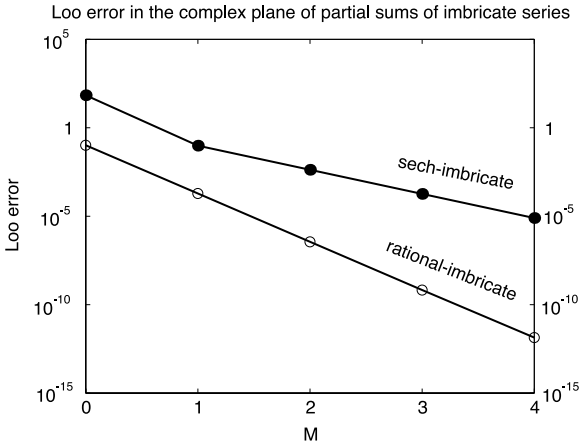

Fig. 4. The maximum pointwise error in the complex domain $\Re(z)\in[0,P/2]$ and $\Im(z)\in[0,P/4]$. Because of the symmetries and periodicities of the cosine lemniscate function, the errors in this one rectangle bound the errors throughout the entire complex plane. Upper curve: errors in $S_M\equiv B\sum_{m=-M}^{M}(-1)^m\ \mathrm{sech}(B(z-mP/2))$. Lower curve: maximum pointwise error in $R_M\equiv A\sum_{m=-M}^{M}\ \cos(B[z-\mathrm{i}mP])/\{(1+q)^2-4q\cos^2(B[z-\mathrm{i}mP])\}$.

2.4. A rational imbricate series

If we repeat the trick of the previous subsection an infinite number of times, that of adding $\Lambda(z-\mathrm{i}mM;p)$ in an analytical form while subtracting its Fourier series, we obtain with $q=\exp(-\pi)$,

$$\mathrm{coslem}(z)=A\sum_{m=-\infty}^{\infty}\frac{\cos(B[z-P\,\mathrm{i}])}{(1+q)^2-4q\cos^2(B[z-\mathrm{i}mP])} \tag{20}$$

where $P=(4/\sqrt{2})K$ is the period in both the real and imaginary directions, $A=4B\sqrt{q}(1-q)$, $B=\pi/(K\sqrt{2})$ and $q=\exp(-\pi)$. In comparison to the classical imbricate series, this series is non-alternating (no factor of $(-1)^m$) and the "stride length" (shift between neighboring copies of the "pattern function") is P rather than $P/2$. Because the cosine functions grow exponentially along the *imaginary* axis, the $|m|$th terms collectively are $O(4\exp(-2|m|\pi))$ or $q^{2|m|}$. Like the standard imbricate series, the rational imbricate series converges uniformly over the entire complex plane. However, it converges much faster than the classical imbricate series—as $q^{2|m|}$ instead of $q^{|m|}$.

If we keep just the $m=0,\pm1$ terms, the difference from coslem(z) is a Fourier series whose coefficients fall as powers of $q^7\sim1/(3.5\times10^9)$! The generalization to more rational terms and Fourier series converging as q^{11}, q^{15}, etc., is obvious (Fig. 3).

Fig. 4 shows the maximum pointwise absolute errors of the partial sums of the two imbricate series in the complex plane. This confirms the geometric convergence of both series [asymptoting to a straight line on a log-linear plot] and the much faster convergence of the new rational imbricate series.

3. Inversion of coslem by transformation and Chebyshev expansion

Without attempting a detailed comparison between many algorithms, we offer some novel methods here.

3.1. A geometrically converging Chebyshev series for the arccoslem function for real argument

Change the variable via

$$u = \cos(1.1981402z) = \cos(Bz) \leftrightarrow Bz = \arccos(u). \tag{21}$$

Using the identity $\cos(n \arccos(u)) = T_n(u)$ for all non-negative integers u where $T_n(u)$ is the nth Chebyshev polynomial, the Fourier series (10) becomes a Chebyshev series in u:

$$F(u) \equiv \text{coslem}\left(\frac{\arccos(u)}{B}\right) = 0.9550060u + 0.0430495T_3(u) + 0.0018605T_5(u) + 0.0000804T_7(u). \tag{22}$$

(The coefficients are the numerical evaluation of the coefficients given symbolically in (10).) The inverse is obtained by solving

$$F(u) - w = 0 \leftrightarrow u(w) = F^{-1}(w). \tag{23}$$

Note that because the range of $F(u)$, like that of the coslem function itself, is $[-1, 1]$ for real $u \in [-1, 1]$, it is sufficient to expand the inverse $u(w)$ as a Chebyshev series on the canonical interval $w \in [-1, 1]$. The Chebyshev interpolation points are

$$w_k \equiv \cos\left(\pi \frac{2k+1}{2N+2}\right), \quad k = 0, 1, 2, \ldots, N \tag{24}$$

where it is convenient to choose N even. Step two is to compute the elements of the $(N+1) \times (N+1)$ interpolation matrix. Define $c_j = 2$ if $j = 0$ and $c_j = 1 \forall j > 0$. Then the elements of the interpolation matrix are

$$\mathbb{I}_{jk} = \frac{2}{c_j(N+1)} \cos\left(j\pi \frac{2k+1}{2N+2}\right). \tag{25}$$

The third step is to compute the grid point values of $u(w)$, the function to be approximated:

$$u_k \equiv u(w_k), \quad k = 0, 1, \ldots, N. \tag{26}$$

We obtained the u_k through the quasi-Newton iteration, beginning with $u_k^0 = w_k$,

$$u_k^{(m+1)} = u_k^{(m)} - (1/0.9550060)\left\{w_k - \sum_{n=1}^{N_{\text{Fourier}}} a_j T_{2j-1}(u_k^{(m)})\right\}, \quad m = 0, 1, 2, \ldots \tag{27}$$

where we have used the simplification that all *even* Fourier cosine coefficients are *zero*.

The last step is to compute the Chebyshev coefficients through a vector–matrix multiplication:

$$b_j = \sum_{k=0}^{N} \mathbb{I}_{jk} f_k, \quad j = 0, 1, 2, \ldots, N. \tag{28}$$

The approximation is

$$\text{coslem}^{-1}(w) \equiv \text{arccoslem}(w) \approx \frac{1}{1.198140\ldots} \arccos\left\{\sum_{j=1}^{N} b_{2j-1} T_{2j-1}(w)\right\} \tag{29}$$

where we have used the simplification that all *even* Chebyshev coefficients are *zero*. (A standard Newton's iteration would converge faster than (27), but is unnecessary for real w where $dF/du(u(w)) \approx 0.955$.) The nonzero coefficients up to machine precision are given in Table 2. We have not attempted to determine the precise accuracy of this approximation, but think it close to machine precision.

It is very common for functions to be singular at the endpoints, but the more complicated strategies described in [34,35] are unnecessary here. For real w, the arccosine transformation completely removes the difficulty (Fig. 5).

3.2. Polynomialization of the cosine lemniscate function to compute the inverse function for complex argument

3.2.1. Symmetries

We adopt the convention that z is always the argument of the cosine lemniscate function while w is always the argument of its inverse.

Because the inverse lemniscate functions are multi-valued, it is helpful to define one branch as the principal branch. Our convention is to let $z_P(w)$ denote the principal branch and to define it to consist of values of z in $\Re(z) \in [0, P/2]$

Table 2
Chebyshev coefficients of $u(w)$ where
$\text{arccoslem}(w) = (1/1.198140234735592207)\arccos(u(w))$.

n	a_{2j-1}
1	1.041273025015855e+00
3	−4.474695745896504e−02
5	3.842272977779399e−03
7	−4.122502528023983e−04
9	4.953025059004821e−05
11	−6.375245469254467e−06
13	8.596024227903476e−07
15	−1.198499024008146e−07
17	1.713797522667450e−08
19	−2.499606609512315e−09
21	3.704152792991182e−10
23	−5.561249292624180e−11
25	8.440899196403051e−12
27	−1.293183424369855e−12
29	1.998980691358305e−13
31	−3.043530044218726e−14
33	6.717630354187090e−15

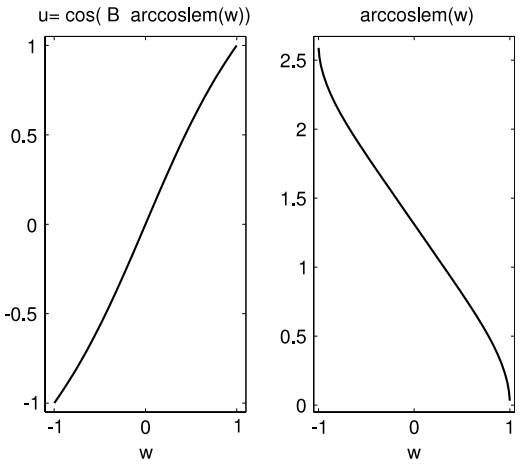

Fig. 5. Right: $\text{arccoslem}(w)$ for real w; this function has square root singularities at $w = \pm 1$ where the function has an infinite slope. Left: In contrast, the function $u = \cos(B\,\text{arccoslem}(w))$ has a geometrically convergent Chebyshev series because it has no singularities for real $w \in [-1, 1]$; the cosine transformation has desingularized the inverse lemniscate function.

and $\Im(z) \in [-P/4, P/4]$. Note that this square occupies just one-fourth of the area of the $P \times P$ period box. The complete branches for all w are

$$\text{arccoslem}(w) = z_P(w) + jP + inP \tag{30}$$
$$= -z_P(w) + jP + inP \tag{31}$$
$$= P/2 - \Re(z_P(w)) + i(-P/2 - \Im(z_P)) + jP + inP \tag{32}$$
$$= -P/2 + \Re(z_P(w)) + i(P/2 + \Im(z_P)) + jP + inP \tag{33}$$

for all integers j and n. The three points in the second, third and fourth lines for $j = n = 0$ give the other branches that lie within the periodic box $[-P/2, P/2] \otimes [-P/2, P/2]$ in the complex z-plane. These relations apply for *all* complex w.

Because of the sixteen fold symmetry within the period box, which is a four fold symmetry within the principal branch square, it is sufficient to plot $\text{arccoslem}(w)$ only in the upper right quadrant of the w-plane, which maps into the square $\Re(z) \in [0, P/4]$ and $\Im(z) \in [0, -P/4]$. Define

$$Z(w) \equiv \text{arccoslem}(|\Re(w)| + \text{i}|\Im(w)|). \tag{34}$$

Then,

$$\text{arccoslem}(|\Re(w)| - \text{i}|\Im(w)|) = \Re(Z) - \text{i}\Im(Z) \tag{35}$$
$$\text{arccoslem}(-|\Re(w)| + \text{i}|\Im(w)|) = P/2 - \Re(Z) + \text{i}\Im(Z) \tag{36}$$
$$\text{arccoslem}(-|\Re(w)| - \text{i}|\Im(w)|) = P/2 - \Re(Z) - \text{i}\Im(Z). \tag{37}$$

If w is in the upper right quadrant, $\Re(w) \in [0,\infty]$ and $\Im(w) \in [0,\infty]$, then the principal branch of this quadrant lies in $\Re(z) \in [0, P/4]$ and $\Im(z) \in [0, -P/4]$. The lower right quadrant maps into $\Re(z) \in [0, P/4] \otimes \Im(z) \in [0, P/4]$. The upper left quadrant in w maps into $\Re(z) \in [P/4, P/2] \otimes \Im(z) \in [0, -P/4]$. The lower left quadrant in w maps into $\Re(z) \in [P/4, P/2] \otimes \Im(z) \in [0, P/4]$.

3.2.2. Low order approximations

The inverse of the cosine lemniscate function, $z = \text{arccoslem}(w)$, is the solution to

$$\text{coslem}(z) - w = 0. \tag{38}$$

Newton's method is easy to implement:

$$z^{(n+1)} = z^{(n)} - \frac{\text{coslem}(z^{(n)}) - w}{\text{dcoslem}(z^{(n)})/\text{dz}}. \tag{39}$$

However, iterative methods require a first guess. We experimented with two low order approximations.

The quadratic approximation is obtained by first substituting just the rational function of the rational-and-Fourier expansion into $\text{coslem}(z) - w = 0$ to obtain

$$0.95322\,\frac{\cos(Bz)}{1.08829 - 0.17285\,\cos^2(Bz)} - w = 0. \tag{40}$$

By substituting $u = \cos(Bz)$ and solving the resulting quadratic equation in u one obtains the "quadratic approximation"

$$\text{arccoslem}(w) = \frac{1}{1.19814}\,\arccos\left\{-\frac{2.75728}{z} \pm \frac{1}{w}\sqrt{7.60259 + 6.29598w^2}\right\}. \tag{41}$$

The plus sign gives the correct principal branch for w in the upper right quadrant. The left panel in Fig. 6 shows that the approximation has an absolute error less than 0.1 over most of the upper right quadrant in w, but there is a small region of larger error near the branch point at $w = i$ where Newton's algorithm needs as many as thirty iterations.

A better approximation is obtained by keeping the next term in (18). This gives the cubic in $u = \cos(Bz)$.

$$P_3(u) = u^3 + c_2u^2 + c_1\,u + c_0 \tag{42}$$

where

$$c_2 = 24.2309399w \tag{43}$$

$$c_1 = 127.32693724 \tag{44}$$

$$c_0 = -152.557431249w. \tag{45}$$

The general solution is, defining

$$\rho = (2/3)\sqrt{c_2^2 - 3c_1}, \qquad \lambda = -((8/27)c_2^3 - (4/3)c_2c_1 + 4c_0)/\rho^3 \tag{46}$$

$$r_k = -c_2/3 + \rho\cos((1/3)\arccos(\lambda) + (2k\pi/3)), \quad k = 0, 1, 2 \tag{47}$$

$$z_k = (1/B)\arccos(r_k), \quad k = 0, 1, 2. \tag{48}$$

We then choose the root with $\Re(z) > 0$, $\Im(z) < 0$, corresponding to the principal branch for w in the upper right quadrant of the w-plane. One minor complication is that the branch cut of the arccosine function in computer libraries is on the real axis for $w > 1$; to avoid an incorrect branch, one can add a tiny positive imaginary part of w, or choose a nonstandard branch of the arccosine when w is real and $w > 1$.

This has an absolute error of less than 0.0001 over most of the domain $\Re(w) \geq 0$ and $\Im(w) \geq 0$ except for again a boundary layer of larger error around $w = i$ (Fig. 6).

Fig. 7 shows that just three or fewer Newton iterations suffice except very close to $w = i$ where five are necessary.

3.3. Tredecic approximation

In a long series of papers, the author has shown how transcendental functions can be "polynomialized" to find their roots [36–44]. The reason that this is a good strategy is that reliable "black box" polynomial rootsolvers are now widely available. Boyd's strategy is to expand $f(u)$ as a Chebyshev series in u, on either one or many intervals, and then find the roots as the eigenvalues of the Chebyshev companion matrix. This strategy is now operational in Trefethen's "Chebfun" extension to Matlab [45]. One limitation is that a Chebyshev series is highly accurate only on the target interval; complex roots of the polynomial are usually poor approximations to those of $f(u)$ except for those very close to the (real) expansion interval.

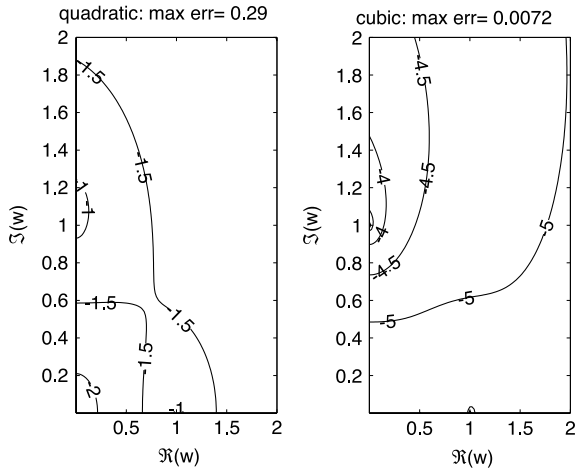

Fig. 6. Left: contours of the base-10 logarithm of the errors in the quadratic approximation. Right: same but for the cubic approximation. The errors in the rest of upper right quadrant of the complex w-plane, not shown, are smaller than those at the top and right of each graph.

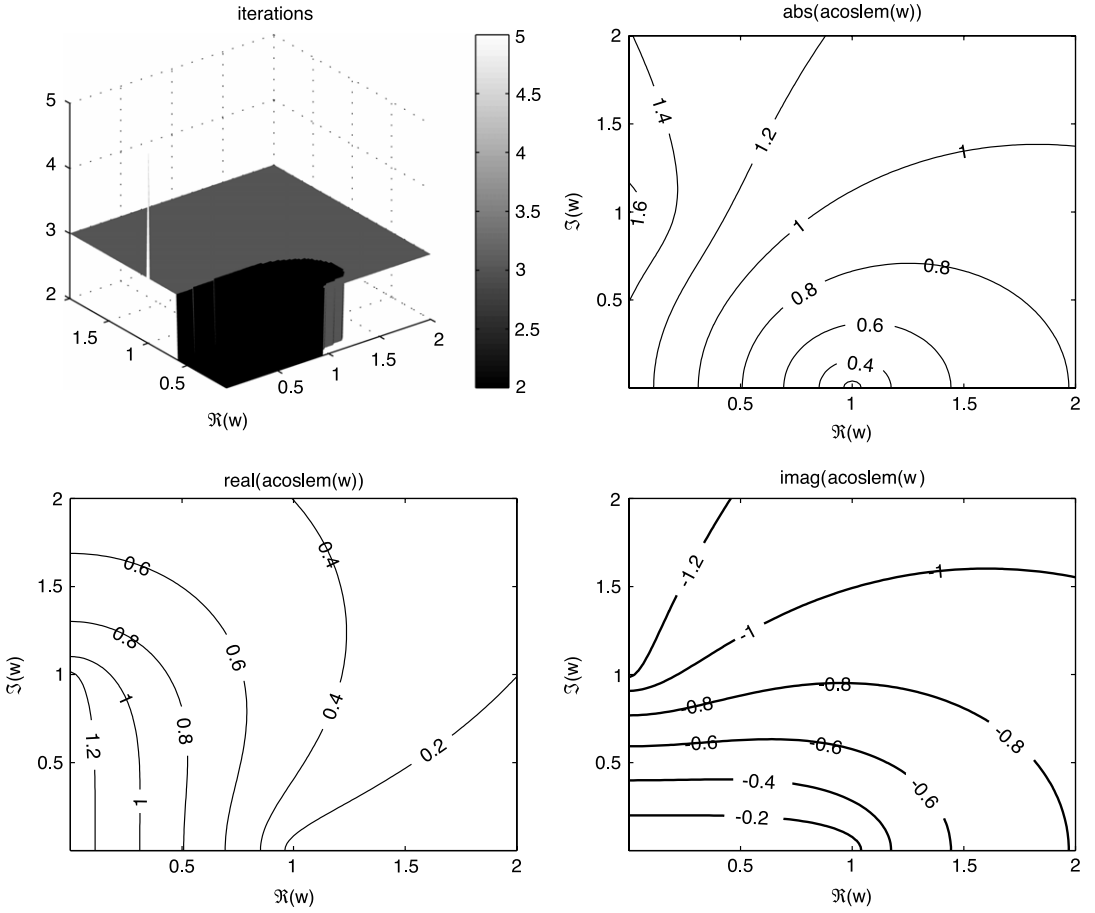

Fig. 7. Upper left: number of iterations required to lower the Newton correction below 10^{-10}, beginning from the cubic approximation. Other three plots: contours of $|z|$, $\Re(z)$ and $\Im(z)$.

A similar strategy can be applied to find the roots of $\text{coslem}(z) - w = 0$ and thus determine $z = \text{arccoslem}(w)$—only better. The rational-plus-Fourier series converges so rapidly that only four Fourier terms suffice to give an approximation to full machine accuracy for real w. (We have already given a direct Chebyshev series for the inverse coslem function that makes rootfinding of any kind unnecessary, but only for *real* w.) If we add just two more terms, however, we obtain an

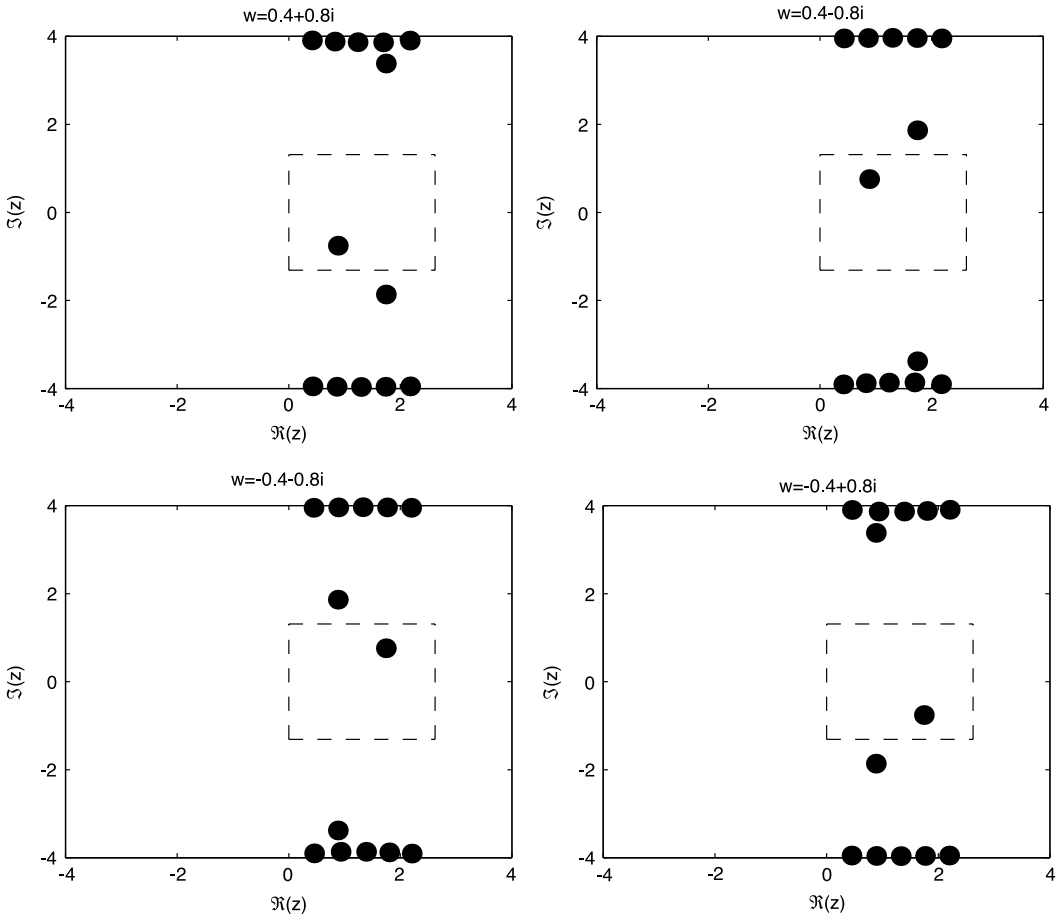

Fig. 8. Roots of the tredecic polynomial in the complex z-plane for four different values of w. The single root in the dashed box is the principal branch of the arccoslem function for that value of w.

approximation which is accurate to about sixteen digits over the entire *complex* strip $\Im(w) \le P/4 = 1.31\ldots$. From knowledge of the roots of $\mathrm{coslem}(z) - w = 0$ within this strip, we can apply double periodicity and symmetries to compute $z = \mathrm{arccoslem}(w)$ in the entire complex plane!

Multiplying the rational-plus-six-Fourier approximation to $\mathrm{coslem}(z) - w = 0$ by the denominator of the rational term and eliminating the cosines by the change of variable $u = \cos(Bz)$ gives a polynomial of degree thirteen in u that we shall dub the "tredecic approximation":

$$\begin{aligned} P_{13}(u) = {} & 1.08829527925925248836\, w - 0.90832045173695339089\, u - 0.17285567305508899910\, wu^2 \\ & - 7.11675748874377388775 \times 10^{-3}\, u^3 - 2.39620478872139259573 \times 10^{-6}\, u^5 \\ & - 7.73427901724042173093 \times 10^{-10}\, u^7 - 2.49620781886680951411 \times 10^{-13}\, u^9 \\ & - 8.05638967796512750996 \times 10^{-17}\, u^{11} - 2.60820305648868108692 \times 10^{-20}\, u^{13}. \end{aligned} \tag{49}$$

The coefficients were computed using forty-digit arithmetic in Maple. This polynomial could be written as a sum of Chebyshev polynomials as in [36,39,42], but this is advantageous in reducing roundoff errors only when u is *real*.

To find the roots in Matlab, merely form the coefficients into a vector **P13** and type *roots*(**P13**). The polynomial has thirteen roots, but after conversion from u to z via $z = (1/B)\mathrm{arcccos}(u)$, most will lie far outside the "strip of accuracy" $\Im(w) \le P/4 = 1.31\ldots$. The final step, therefore, is to test the roots and only accept the unique root within the box $z_P \in [0, P/2] \otimes [-P/4, P/4]$. From this single root, $z_P(w)$, all the other branches of the multi-valued inverse cosine lemniscate (lemniscate integral) can be found by applying (30)–(33).

Fig. 8 illustrates the principal branch and the spurious roots for four different values of w, each in a different quadrant of the complex w-plane.

This polynomialize/polyrootfind/test strategy is simple to program and very robust. It has the drawback that its formal operation count is higher than a simple Newton iteration; we are computing thirteen zeros and discarding all but one. The most common way to compute polynomial roots, the companion matrix strategy which is the default in Matlab, costs $O(10\ N^3)$ floating point operation where N is the matrix size, here thirteen. It is nevertheless remarkable that a

transcendental function is, after three centuries, reduced to a polynomial proxy that is indistinguishable from the real thing to within machine precision everywhere in a strip in the complex plane.

4. Summary

It is remarkable that it is possible to say anything new about functions which have been studied by James Bernoulli, Euler, Gauss, Legendre, Abel, Jacobi and Ramanujan. Nevertheless, we have been able to find exponentially convergent formulas to compute the cosine lemniscate function for all complex z. We have also obtained a novel Chebyshev series, accurate to almost full machine precision, and easily extended to arbitrary precision, for computing the lemniscate integral for *real* z. Furthermore, we have "polynomialized" the lemniscate integrate by showing that it can be computed for *complex* z by finding the roots of an algebraic polynomial of low degree.

We do not wish to overclaim. Maple and Mathematica can already evaluate the lemniscate integral in the complex plane as a special case of elliptic integrals. The Landen transformation and the arithmetic–geometric mean are powerful tools for computing elliptic functions and integrals. It is therefore not sensible to claim that we offer ways to calculate the previously incalculable. Nevertheless, we believe it is still worthwhile, for such heavily studied functions, to find new series and approximations that are superior to previously known expansions.

The new Fourier series for the cosine lemniscate function is a good illustration of Darboux's Principle for Fourier series, which asserts that each singularity z_s in the strip $\Re(z) \in (-P/2, P/2]$ makes a contribution proportional to $\exp(-n(2\pi/P)\,|\Im(z_s)|)$ to the nth Fourier coefficient as $|n| \to \infty$. Thus, the coefficient of $\cos([2n-1](2\pi/P)z)$ in the classical Fourier series converges proportionally to $q^{n-1/2} = \exp(-(n-1/2)\pi)$ because of the poles of the cosine lemniscate function at $|\Im(z)| = \pm \mathrm{i}P/4$. The rational-plus-Fourier series converges much faster because the function $f(z) \equiv \mathrm{coslem}(z) - A\cos(Bz)/((1+q)^2 - 4q\cos^2(Bz))$ is free of poles out to $|\Im(z)| = 3P/4$. Again consistent with Darboux's Principle, each term in the series of odd cosines for $f(z)$ is smaller than its predecessor by a factor of $q^3 = \exp(-2(2\pi/P)(3P/4)) = \exp(-3\pi)$ versus $q = \exp(-\pi)$ for the classical series.

The fact that every periodic function has a non-Fourier representation as the periodization of a "pattern" function, a so-called "imbricate" series, is a consequence of the nineteenth century Poisson Summation Theorem. Unfortunately, this folklore is rarely discussed in class, even in classes targeted at engineering students. The cosine lemniscate function and Jacobian elliptic functions embody this folklore squared in the sense that the periodicity in both the real and imaginary directions gives rise to *two* imbricate series. The new imbricate series of rational functions of the cosine, each copy identical except for translation along the *imaginary* z-axis, converges faster than the long-known series which is the periodization-for-real-z of the sech function.

In this article, we have limited our discussion to the lemniscate functions since this case alone arose in the application that motivated this work. However, the elliptic cosine function for general modulus also is doubly periodic with a doubly infinite lattice of simple poles. This implies that the new ideas developed here are equally applicable to elliptic functions in general. Deriving a rational-plus-Fourier series and an "inverse-by-polynomial" for general elliptic functions is left for the future.

Acknowledgements

This work was supported by NSF Grants OCE998636, OCE0451951 and ATM 0723440. I thank the reviewer for detailed comments and suggestions.

Appendix. Identities

The following are taken from Sogo [46], Ayoub [2], Boyd [24,47,25,26] and Siegel [32].

$$\mathrm{coslem}^2(x) + \mathrm{sinlem}^2(x) + \mathrm{sinlem}^2(x)\mathrm{coslem}^2(x) = 1 \tag{50}$$

$$\mathrm{sinlem}(2x) = \frac{2\mathrm{sinlem}(x)\sqrt{1-\mathrm{sinlem}^4(x)}}{1+\mathrm{sinlem}^4(x)} \tag{51}$$

$$\mathrm{sinlem}^2([1+i]x) = \frac{(1+i)\mathrm{sinlem}(x)}{\sqrt{1-\mathrm{sinlem}^4(x)}} \tag{52}$$

$$\mathrm{sinlem}^2(x) = \frac{1-\mathrm{coslem}^2(x)}{1+\mathrm{coslem}^2(x)} \tag{53}$$

$$\mathrm{sinlem}(x+y) = \frac{\mathrm{sinlem}(x)\mathrm{coslem}(y) + \mathrm{sinlem}(y)\mathrm{coslem}(x)}{1-\mathrm{sinlem}(x)\mathrm{sinlem}(y)\mathrm{coslem}(x)\mathrm{coslem}(y)} \tag{54}$$

$$\mathrm{coslem}(x+y) = \frac{\mathrm{coslem}(x)\mathrm{coslem}(y) - \mathrm{sinlem}(x)\mathrm{sinlem}(y)}{1-\mathrm{sinlem}(x)\mathrm{sinlem}(y)\mathrm{coslem}(x)\mathrm{coslem}(y)} \tag{55}$$

$$\mathrm{coslem}(2x) = \frac{\mathrm{coslem}^4(x) + 2\mathrm{coslem}^2(x) - 1}{1 + 2\mathrm{coslem}^2(x) + \mathrm{coslem}^4(x)} \tag{56}$$

$$\mathrm{coslem}(3x) = \frac{\mathrm{coslem}^8(x) + 6\mathrm{coslem}^4(x) - 3}{1 + 6\mathrm{coslem}^4(x) - 3\mathrm{coslem}^8(x)} \tag{57}$$

$$\mathrm{arccoslem}(r) = 2\mathrm{arccoslem}(u), \qquad r^2 \equiv \frac{4u^2(1-u^4)}{(1+u^4)^2} \quad \text{[Count Fagnano, 1718]} \tag{58}$$

$$\mathrm{arccoslem}(r) = \mathrm{arccoslem}(u) + \mathrm{arccoslem}(v), \quad r \equiv \frac{u\sqrt{1-v^4} + v\sqrt{1-u^4}}{1+u^2v^2} \quad \text{[Euler, 1753]} \tag{59}$$

$$u_{xx} + 2u^3 = 0, \qquad u(x) = 0.8346\,\mathrm{coslem}(0.8346x) \tag{60}$$

$$u_{xxx} + uu_x = 0, \quad u = 2.08975\,\mathrm{coslem}^2(0.4173x). \tag{61}$$

References

[1] J. Gray, Worlds Out of Nothing: A Course in the History of Geometry in the 19th Century, Springer, New York, 2007.
[2] R. Ayoub, The lemniscate and Fagnano's contributions to elliptic integrals, Arch. Hist. Exact Sci. 29 (1984) 131–149.
[3] G.M. Scarpello, D. Ritelli, Elliptic integral solutions of spatial elastica of a thin straight rod bent under concentrated terminal forces, Meccanica 160 (2006) 976–985.
[4] R. Sridharan, Physics to mathematics: from lintearia to lemniscate I, Resonance 9 (2004) 21–29.
[5] R. Sridharan, From lintearia to lemniscate II: Gauss and Landen's work, Resonance 9 (2004) 11–20.
[6] A. Rice, In search of the 'birthday' of elliptic functions, Math. Intelligencer 30 (2008) 48–56.
[7] R. Levien, From spiral to spline optimal techniques in interactive curve design, Ph.D. Dissertation, University of California at Berkeley, Department of Engineering-Electrical Engineering and Computer Science, 2009, p. 253.
[8] T.A. Driscoll, L.N. Trefethen, Schwarz–Christoffel Mapping, in: Cambridge Monographs on Applied and Computational Mathematics, vol. 8, Cambridge University Press, Cambridge, 2002.
[9] H.A. Schwarz, Conforme abbildung der oberflache eines tetraeders auf die oberflache einer kugel, J. Reine Angew. Math. 70 (1869) 121–136. Also in Schwarz' Collected Works, vol. II, pp. 84–101.
[10] N. Kurt, Solution of the two-dimensional heat equation for a square in terms of elliptic functions, J. Franklin Inst. 345 (2007) 303–317.
[11] P. Amore, Solving the Helmholtz equation for membranes of arbitrary shape: numerical results, J. Phys. A: Math. Theor. 41 (2008) 265206.
[12] J.P. Boyd, F. Yu, Comparing six spectral methods for interpolation and the Poisson equation in a disk: radial basis functions, Logan–Shepp ridge polynomials, Fourier–Bessel, Fourier–Chebyshev, Zernike polynomials, and double Chebyshev series, J. Comput. Phys. (2009) (submitted for publication).
[13] C. Peirce, A quincuncial projection of the sphere, Amer. J. Math. 2 (1879) 394–396.
[14] O.S. Adams, Conformal projection of the sphere within a square, Special Publication 153, US, Coast and Geodetic Survey, Washington, DC, 1929. 16 pp. Available as PDF from the National Oceanic and Atmospheric Administration.
[15] L.P. Lee, Conformal projections based on elliptic functions, Cartographica 13 (1976) Monograph 16, Supplement No. 1 to Canadian Cartographer.
[16] J.P. Snyder, Flattening the Earth, University of Chicago, Chicago, 1993.
[17] B.C. Berndt, S. Bhargava, Ramanujan's inversion formulas for the lemniscate and allied functions, J. Math. Anal. Appl. 160 (1991) 504–524.
[18] M. Abramowitz, I.A. Stegun, Handbook of Mathematical Functions, Dover, New York, 1965.
[19] S. Leble, Quantum corrections to static solutions of the sine-Gordon and Nahm models via a generalized zeta function, Theoret. and Math. Phys. 160 (2009) 976–985.
[20] J.P. Boyd, Cnoidal waves as exact sums of repeated solitary waves: new series for elliptic functions, SIAM J. Appl. Math. 44 (1984) 952–955.
[21] R. Grimshaw (Ed.), Solitary Waves, WIT Press, Southampton, United Kingdom, 2007.
[22] M. Remoissenet, Waves Called Solitons: Concepts and Experiments, 3rd ed., Springer-Verlag, New York, 1991.
[23] J.P. Boyd, Weakly Nonlocal Solitary Waves and Beyond-All-Orders Asymptotics: Generalized Solitons and Hyperasymptotic Perturbation Theory, in: Mathematics and its Applications, vol. 442, Kluwer, Amsterdam, 1998, p. 608.
[24] J.P. Boyd, Theta functions, Gaussian series, and spatially periodic solutions of the Korteweg–de Vries equation, J. Math. Phys. 23 (1982) 375–387.
[25] J.P. Boyd, New directions in solitons and nonlinear periodic waves: polycnoidal waves, imbricated solitons, weakly non-local solitary waves and numerical boundary value algorithms, in: T.-Y. Wu, J.W. Hutchinson (Eds.), Advances in Applied Mechanics, in: Advances in Applied Mechanics, vol. 27, Academic Press, New York, 1989, pp. 1–82.
[26] J.P. Boyd, Planetary-scale solitary waves, in: R. Grimshaw (Ed.), Solitary Waves in Fluids, WIT Press, Southampton, United Kingdom, 2007, pp. 125–158.
[27] J.P. Boyd, Solitons from sine waves: analytical and numerical methods for non-integrable solitary and cnoidal waves, Physica D 21 (1986) 227–246.
[28] J.P. Boyd, Periodic solutions generated by superposition of solitary waves for the quarticly nonlinear Korteweg–de Vries equation, Z. Angew. Math. Phys. 40 (1989) 940–944.
[29] Y. Yamamoto, E.I. Takizawa, On a solution on non-linear time-evolution equation of fifth order, J. Phys. Soc. Japan 50 (1981) 1421–1422.
[30] K. Kano, T. Nakayama, An exact solution of the wave equation $u_t + uu_x - u_{5x} = 0$, J. Phys. Soc. Japan 50 (1981) 361–362.
[31] M. Takaoka, Pole distribution and steady pulse solution of the fifth order Korteweg–de Vries equation, J. Phys. Soc. Japan 58 (1889) 73–81. Addendum, vol. 58, p. 3028.
[32] C.L. Siegel, Topics in Complex Variable Theory, vol. 1, Wiley-Interscience, New York, 1969.
[33] J.P. Boyd, Chebyshev and Fourier Spectral Methods, 2nd ed., Dover, Mineola, New York, 2001, 665.
[34] J.P. Boyd, R. Visser, Rootfinding through global Newton iteration and Chebyshev polynomials for the gain of a balanced oscillator, Math. Comp. 182 (2006) 166–174.
[35] J.P. Boyd, Chebyshev expansion on intervals with branch points with application to the root of Kepler's equation: a Chebyshev–Hermite–Padé method, J. Comput. Appl. Math. 223 (2009) 693–702.
[36] J.P. Boyd, A Chebyshev polynomial interval-searching method (Lanczos economization) for solving a nonlinear equation with application to the nonlinear eigenvalue problem, J. Comput. Phys. 118 (1995) 1–8.
[37] J.P. Boyd, Computing zeros on a real interval through Chebyshev expansion and polynomial rootfinding, SIAM J. Numer. Anal. 40 (2002) 1666–1682.
[38] J.P. Boyd, Computing real roots of a polynomial in Chebyshev series form through subdivision, Appl. Numer. Math. 56 (2006) 1077–1091. (errata); $(-1)a_{j-1}/a_N$ in the last line of (7) should be $(-1)a_{j-1}/(2a_N)$.
[39] J.P. Boyd, Polynomialization of Kepler's equation through Chebyshev polynomial expansion of the sine: a non-iterative rootfinder, Appl. Numer. Math. 57 (2007) 12–18.

[40] J.P. Boyd, Computing the zeros of a Fourier series or a Chebyshev series or general orthogonal polynomial series with parity symmetries, Comput. Math. Appl. 54 (2007) 336–349.
[41] J.P. Boyd, Computing real roots of a polynomial in Chebyshev series form through subdivision with linear testing and cubic solves, Appl. Math. Comput. 174 (2006) 1642–1648.
[42] J.P. Boyd, D.H. Gally, Numerical experiments on the accuracy of the Chebyshev–Frobenius companion matrix method for finding the zeros of a truncated series of Chebyshev polynomials, J. Comput. Appl. Math. 205 (2007) 281–295.
[43] J.P. Boyd, Computing the zeros, maxima and inflection points of Chebyshev, Legendre and Fourier series: solving transcendental equations by spectral interpolation and polynomial rootfinding, J. Engrg. Math. 56 (2006) 203–219. (errata); $(-1)a_{j-1}/a_N$ in the last line of (2) should be $(-1)a_{j-1}/(2a_N)$.
[44] J.P. Boyd, A test, based on conversion to the Bernstein polynomial basis, for an interval to be free of zeros applicable to polynomials in Chebyshev form and to transcendental functions approximated by Chebyshev series, Appl. Math. Comput. 188 (2007) 1780–1789.
[45] Z. Battles, L.N. Trefethen, An extension of Matlab to continuous functions and operators, SIAM J. Sci. Comput. 25 (2004) 1743–1770.
[46] K. Sogo, Inverse problem in chaotic map theory, Chaos Solitons Fractals 41 (2009) 1817–1822.
[47] J.P. Boyd, Equatorial solitary waves. Part 5. Initial value experiments, co-existing branches and tilted-pair instability, J. Phys. Oceanogr. 32 (2002) 2589–2602.